

Supplemental Information

Single-cell transcriptome analysis of xenotransplanted human retinal organoids defines two migratory cell populations of nonretinal origin

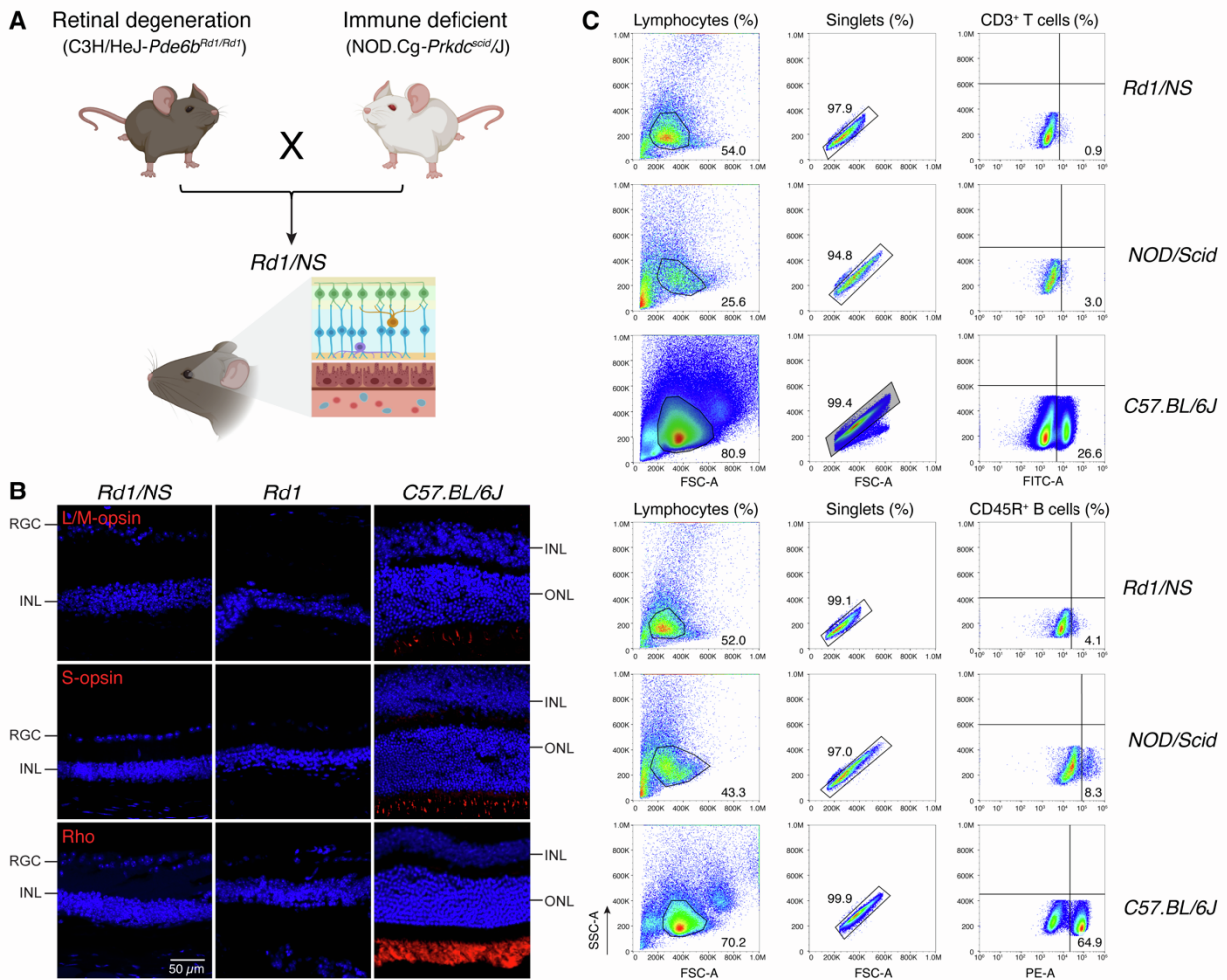
Ying V. Liu, Clayton P. Santiago, Akin Sogunro, Gregory J. Konar, Ming-wen Hu, Minda M. McNally, Yu-chen Lu, Miguel Flores-Bellver, Silvia Aparicio-Domingo, Kang V. Li, Zhuo-lin Li, Dzhalal Agakishiev, Sarah E. Hadyniak, Katarzyna A. Hussey, Tyler J. Creamer, Linda D. Orzolek, Derek Teng, M. Valeria Canto-Soler, Jiang Qian, Zheng Jiang, Robert J. Johnston Jr., Seth Blackshaw, and Mandeep S. Singh

1 **Supplementary Materials**

2
3 **Single-cell transcriptome analysis of xenotransplanted human retinal**
4 **organoids defines two migratory cell populations of nonretinal origin**

5
6 Ying V. Liu, *et al.*

7
8
9 **Supplemental Figure 1**



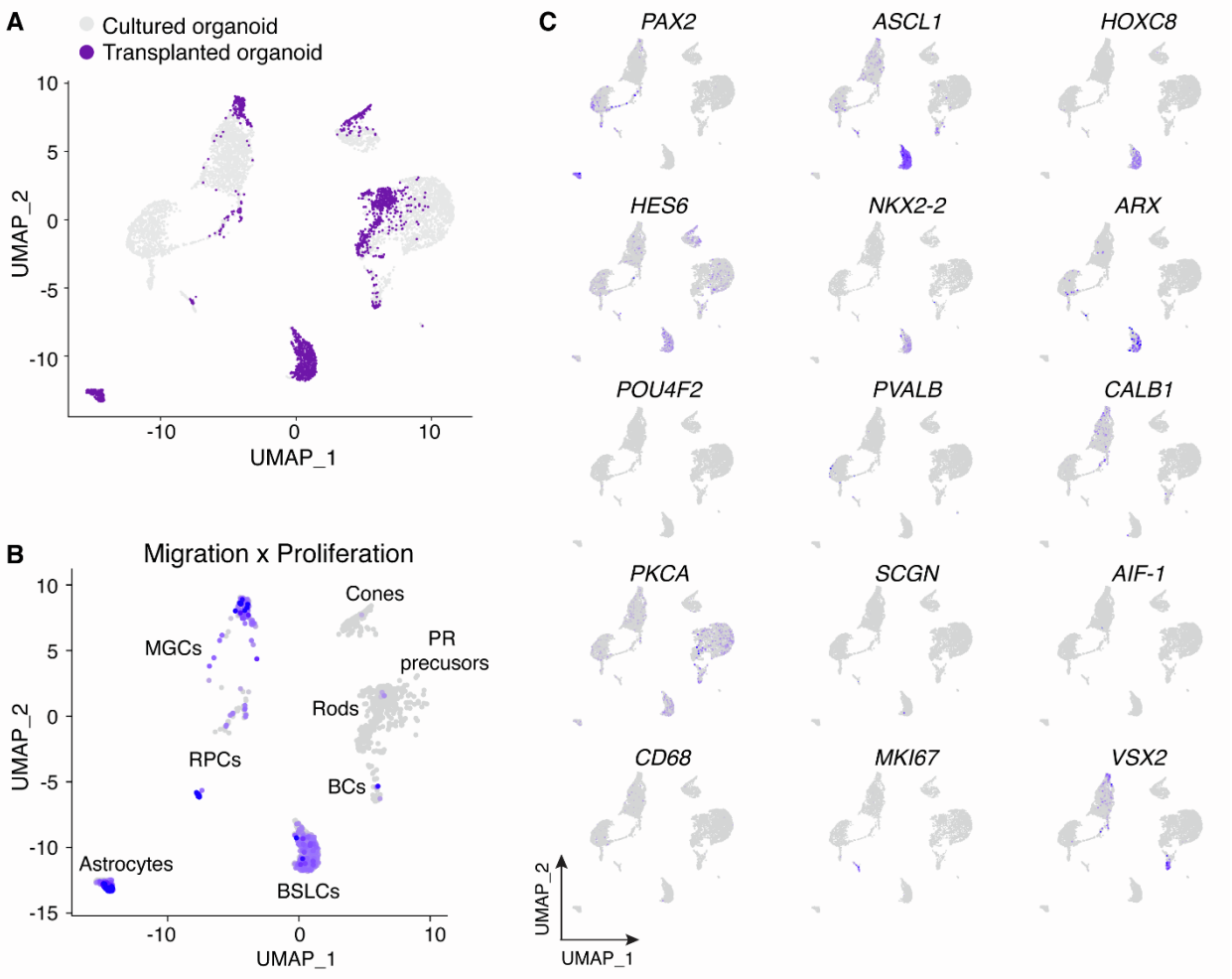
11
12
13 **Fig. S1. Breeding and phenotyping of the recipient *Rd1/NS* mice.** (A) Schematic showed the
14 recipient *Rd1/NS* mice were generated by crossbreeding C3H/HeJ-*Pde6b^{Rd1/Rd1}* (*Rd1*) and
15 NOD.Cg-*Prkdc^{scid}/J* (*NOD/Scid*) mice. (B) IHC staining showed fully degenerated photoreceptor
16 cells and negative expression of L/M-opsin, S-opsin, and Rhodopsin (Rho) in adult *Rd1/NS* mice

17 and *Rd1* mice. *C57.BL/6J* mice served as *wild-type* controls. (C) Flow cytometry analysis showed
18 the deficiency of CD3⁺ T cells and CD45R⁺ B cells in *Rd1/NS* mice, corresponding to the immune
19 deficient phenotype of *NOD/Scid* mice. *C57.BL/6J* mice served as *wild-type* controls. N= 4 eyes
20 per group.

21 Supplemental Figure 2

22

23

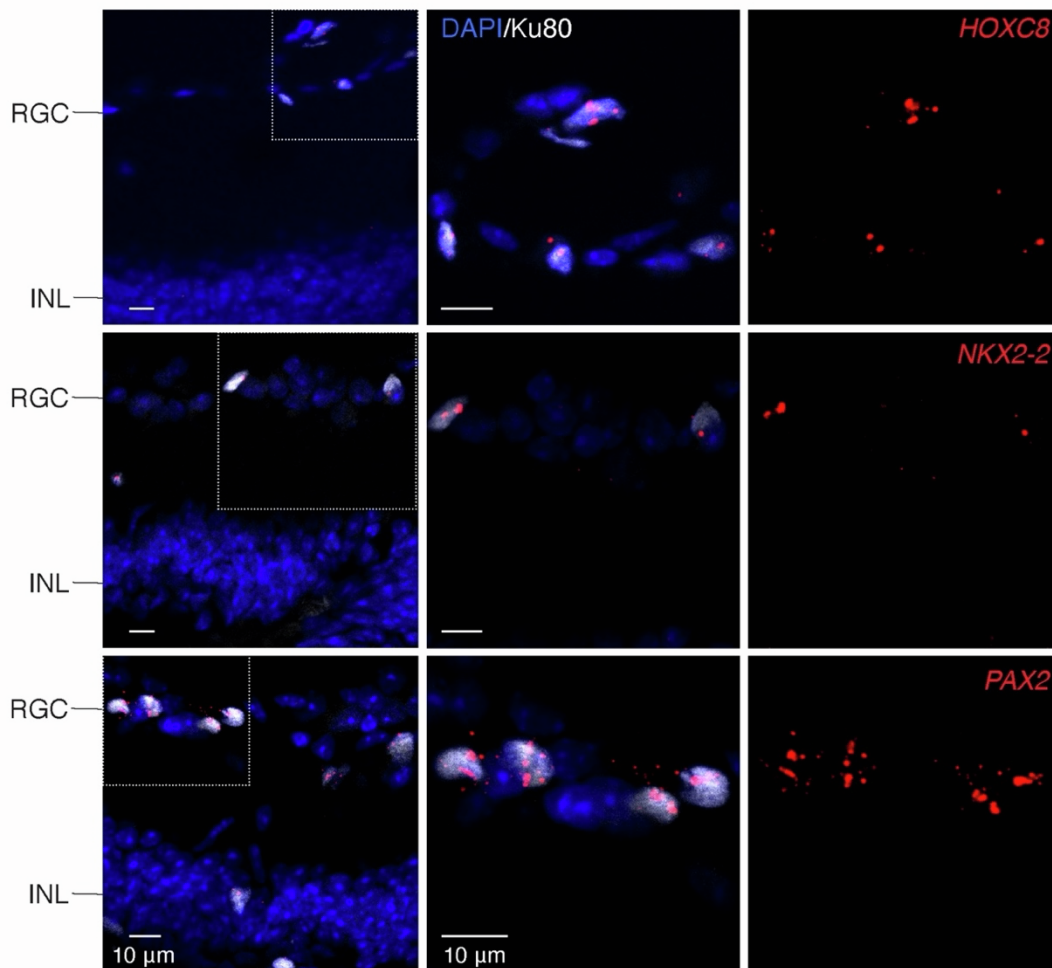


24

25

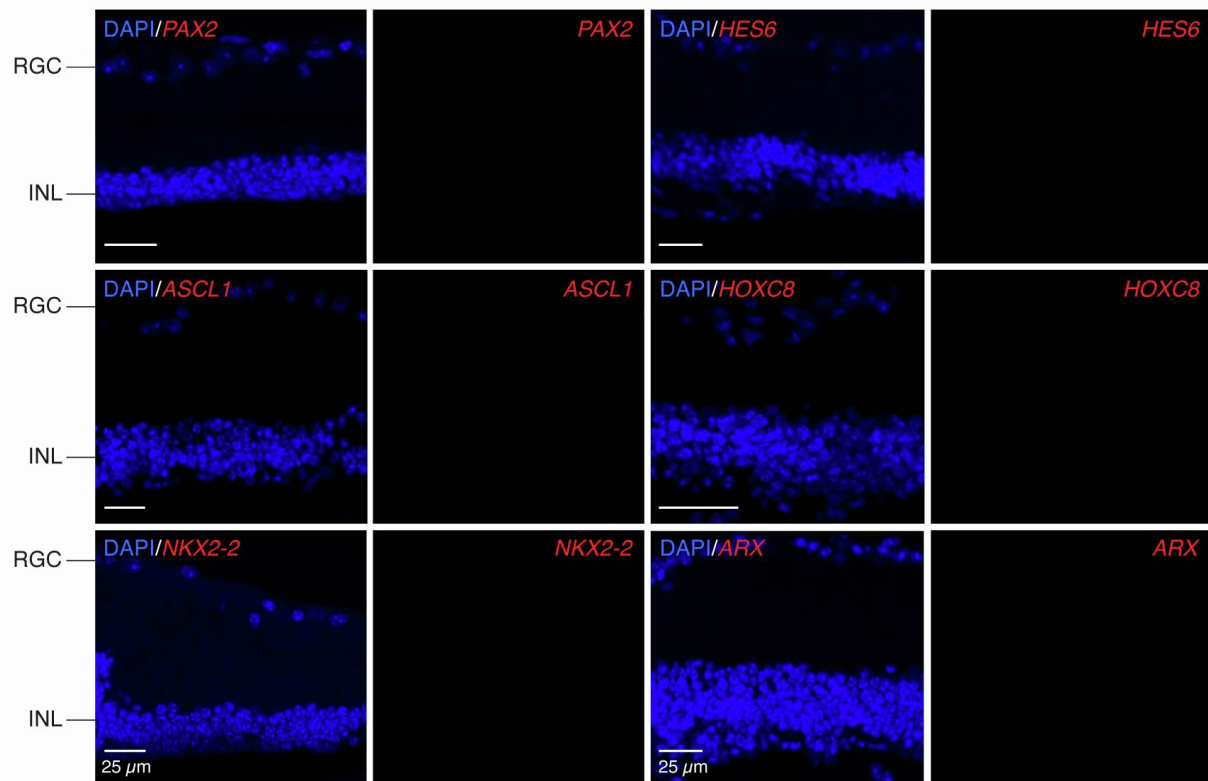
26 **Fig. S2. UMAP plots of migration and proliferation cell clusters. (A)** UMAP plot colored cell
27 clusters of cultured (grey, n=2 organoids from one batch) and transplanted retinal organoids
28 (purple, n=3 transplanted eyes). **(B)** UMAP plot colored cell clusters sharing transcriptomic
29 characteristics of migration and proliferation. **(C)** UMAP plots displayed the expression of marker
30 genes in cell clusters of transplanted and cultured retinal organoids.

31 **Supplemental Figure 3**
32



33
34 **Fig. S3. Human iPSC donor-derived migratory cells include astrocytes and brain/spinal**
35 **cord-like neural precursors.** Migratory cells from human iPSC-derived retinal organoid grafts
36 (n=3 organoids from one iPSC batch, distinct from the H9 ESC-derived organoids used in Fig. 1-
37 7, Fig. S1-S2, and Fig. S5-S6) were detected in the RGC layer and INL of recipient mouse retinae
38 by human nuclear specific antibody Ku80 staining. RNAscope staining showed migratory cells
39 expressing markers of BSL cells (*HOXC8*, *NKX2-2*) and astrocytes (*PAX2*), consistent with the
40 characteristics of those migratory cells in *Crx:tdTomato*⁺ hESC-derived retinal organoid grafts.
41 *Abbreviation: RGC: retinal ganglion cell layer; INL: inner nuclear layer.*

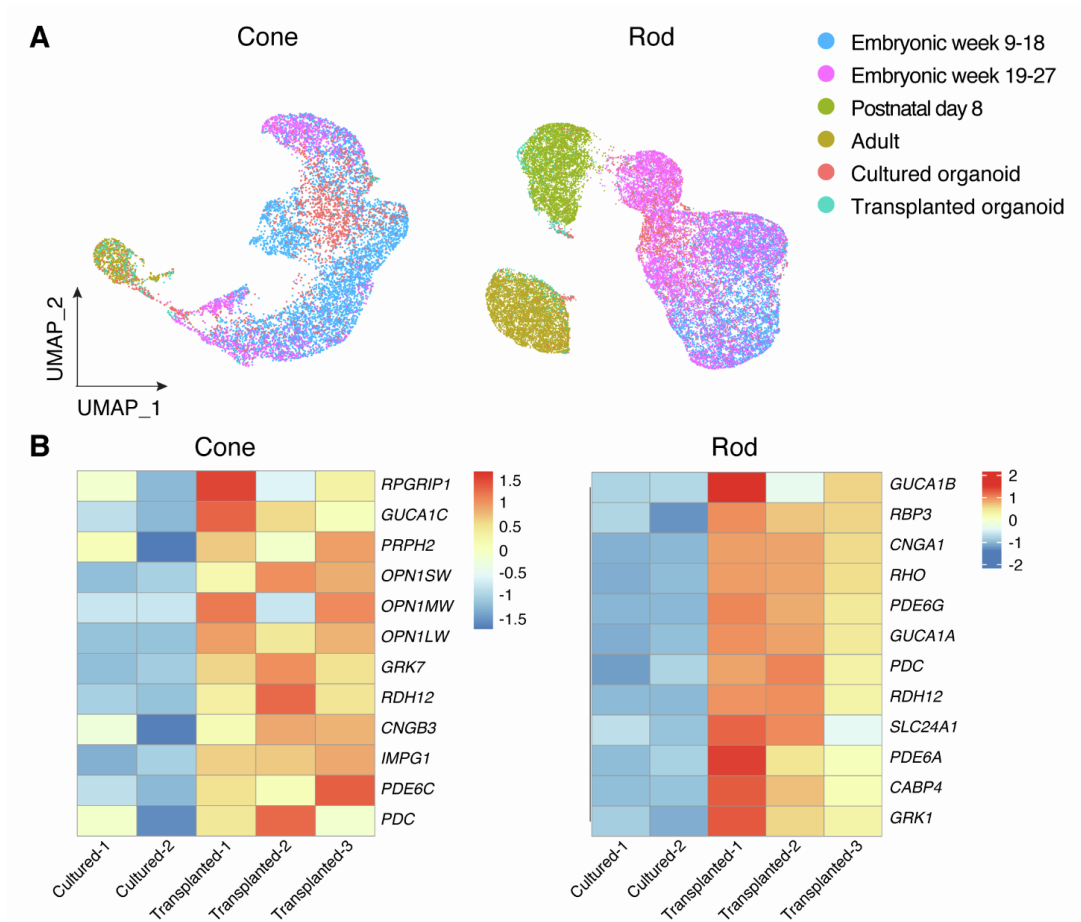
42 Supplemental Figure 4
43



44
45 **Fig. S4. RNAscope staining of human astrocyte and BSL on non-transplanted *Rd1/NS***
46 **control mice.** Cryosections of non-transplanted *Rd1/NS* mice were stained with human probes of
47 astrocyte (*PAX2*) and BSL cells (*HES6*, *ASCL1*, *HOXC8*, *NKX2-2*, *ARX*). None of these human
48 genes were detected in non-transplanted *Rd1/NS* mice retinæ. *Abbreviation: RGC: retinal*
49 *ganglion cell layer; INL: inner nuclear layer.*

50

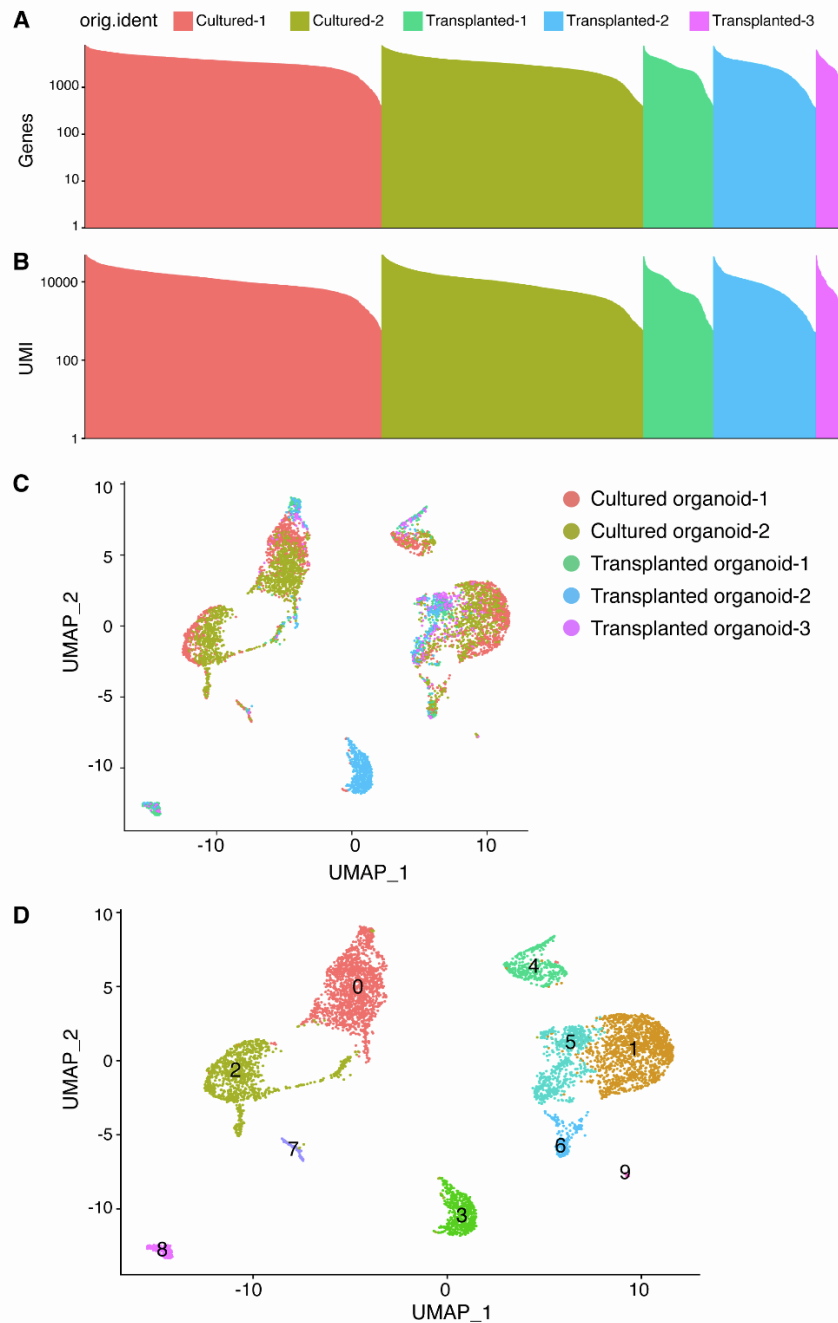
51 Supplemental Figure 5
52



53
54 **Fig. S5. Upregulation of cone and rod marker genes in transplanted retinal organoids. (A)**
55 UMAP plots showed cells colored by sample libraries, including human retina developmental
56 datasets (cone: n = 7,654 cells, rod: n = 25,186 cells), cultured retinal organoids (cone: n =1,639
57 cells, rod: n=1,469 cells, collecting from two organoids in one batch), and transplanted retinal
58 organoids (cone: n=210 cells, rod: n =504 cells, collecting from three transplanted eyes). **(B)**
59 Heatmaps demonstrated the upregulation of marker genes specific for cone and rod photoreceptors
60 in transplanted retinal organoids (including three independent replicates “Transplanted-1,
61 Transplanted-2, Transplanted-3”), compared to cultured retinal organoids (including two
62 independent replicates “Cultured-1, Cultured-2” from one batch).

63 Supplemental Figure 6

64



65

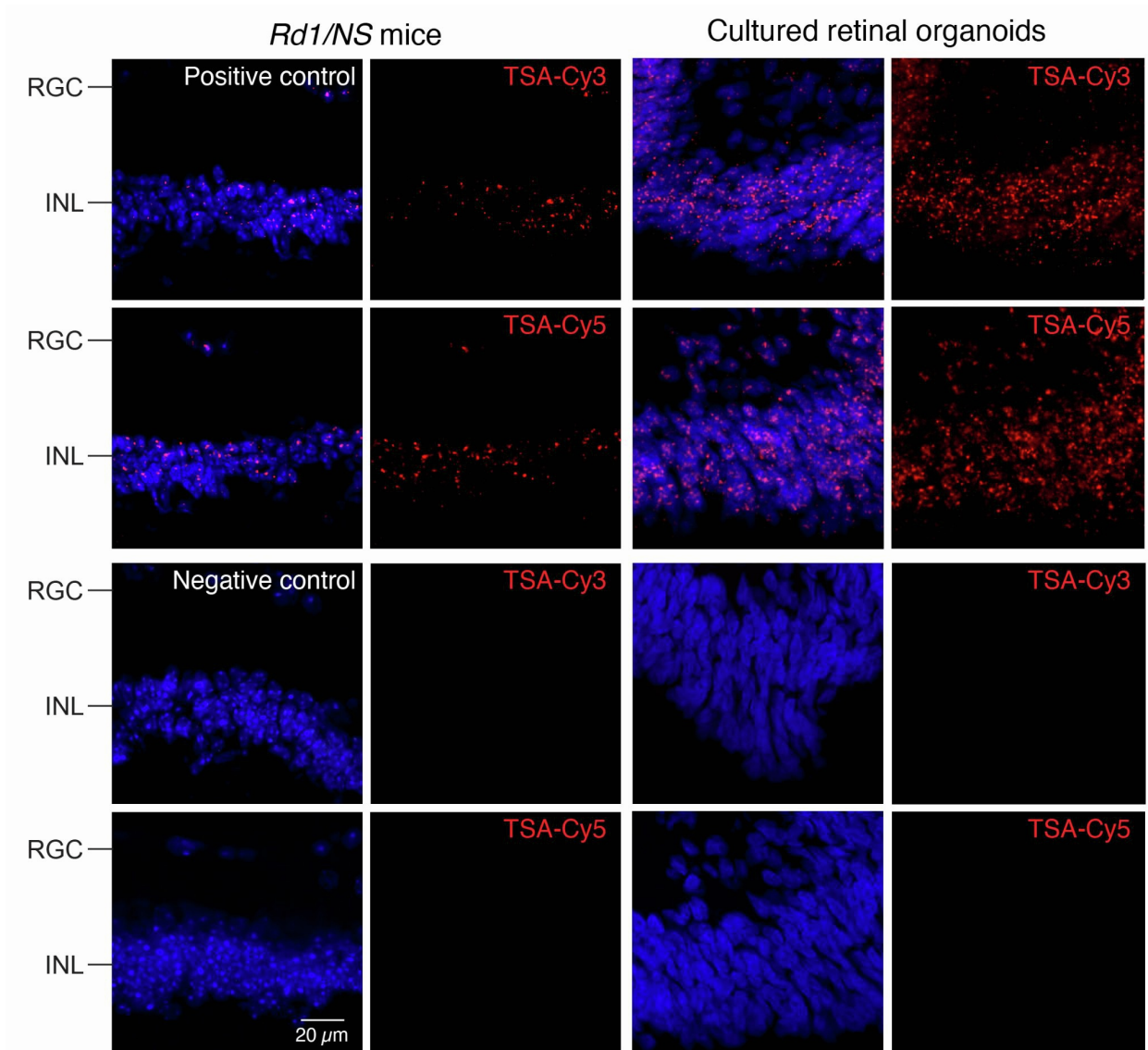
66 **Fig. S6. Quality control of scRNA-seq data. (A)** Number of genes and **(B)** unique molecular

67 identifiers (UMI) per cell. Each bar is a cell and is colored by the sample library and ordered

68 along the x-axis in descending order. **(C)** UMAP plot showing cells colored by sample library.

69 **(D)** UMAP plot showing 10 (0-9) transcriptionally distinct cell clusters.

70 Supplemental Figure 7
71



72
73
74 **Fig. S7. RNAscope staining of positive and negative control probes.** Cryosections of non-
75 transplanted *Rd1/NS* mice and cultured retinal organoids were stained with 3-plex positive and
76 negative control probes in combination with TSA-Cy3 or TSA-Cy5 fluorophores. Positive probes
77 target common housekeeping genes *PPIB* (Cy3) and *POLR2A* (Cy5). Negative probe targets the
78 bacterial *dapB* gene.

79
80

81 **Table S1. BE6.2 media and long-term retina media (LTR) for Crx:tdTomato⁺ retinal**
 82 **organoids.**
 83

Reagent	Concentration	Source	Catalog Number
BE6.2 media			
DMEM	—	Gibco	11885084
B27 minus vitamin A	2%	Gibco	12587010
Glutamax	1%	Gibco	35050061
NEAA	1%	Gibco	11140050
Sodium pyruvate	1mM	Gibco	11360070
NaCl	0.87 mg/mL	Sigma-Aldrich	S9888
E6 supplement	2.5%		
Insulin	970 ug/mL	Roche	11376497001
Holo-transferrin	535 ug/mL	Sigma-Aldrich	T0665
L-ascorbic acid	3.20 mg/mL	Sigma-Aldrich	A8960
Sodium selenite	0.7 ug/mL	Sigma-Aldrich	S5261
long-term retina (LTR) media			
DMEM	—	Gibco	11885084
F12	25%	Gibco	11765062
B27	2%	Gibco	17504044
NEAA	1%	Gibco	11140050
Fetal bovine serum	10%	Gibco	16140071
Sodium pyruvate	1mM	Gibco	11360070
Glutamax	1%	Gibco	35050061
Taurine	1 mM	Sigma-Aldrich	T-8691

84

85
86

Table S2. Retinal organoid culturing media using hiPS cell line.

Reagent	Concentration	Source	Catalog Number
Neural Induction Media (NIM) (Day 3-Day 15)			
DMEM/F12 (1:1)	—	Life Technologies	11330-057
100x N2 Supplement	1% (v/v)	Life Technologies	17502-048
HEPARIN (stock as 1mg/mL in DMEM, 0.1%)	2 ug/mL	Sigma	H3149-100
100x MEM-NEAA	0.01	Life Technologies	11140050
Retinal Differentiation Media (RDM) (Day 16-Day 30)			
DMEM	—	Life Technologies	11330-057
F12	—	Life Technologies	11965
50x B27 (without Vit A)	1x	Life Technologies	11765
100x Antibiotic and Antimycotic	1x	Life Technologies	12587-010
100x MEM-NEAA	1x	Life Technologies	15240
RC2 (Day 30-Day 91)			
DMEM	----	Life Technologies	11965
F12	----	Life Technologies	11765
50x B27 (without Vit A)	1x	Life Technologies	12587010
100x Antibiotic and Antimycotic	1x	Life Technologies	15240
100x MEM-NEAA	1x	Life Technologies	11140050
FBS	10%	Gibco or Atlanta Biologicals	S11150
100x Glutamax	1x	Life Technologies	35050061
1000x Taurine (100mM)	100 uM	Sigma	T0625

Retinoic Acid (directly add RA to cells when changing media)	0.5-1 uM	Sigma-Aldrich	R2625
RC1 (>Day 91)			
DMEM/F12-Glutamax	----	Life Technologies	10565-018
100x N2 Supplement	1% (v/v)	Life Technologies	17502-048
100x Antibiotic and Antimycotic	1x	Life Technologies	15240
100x NEAA	1x	Life Technologies	11140050
FBS	10%	Atlanta Biologics	S11150
1000x Taurine (100mM)	100 uM	Sigma	T0625
Retinoic Acid (directly add RA to cells when changing media)	0.5 uM	Sigma-Aldrich	R2625

87

88 **Table S3. Forward and reverse primer sequences used for mice genotyping.**

89

Gene	F primer (5' to 3')	R primer (5' to 3')
<i>Rd1 Wild type</i>	ACTCTGTGGCCTCAAAGATA CATC	TGCAGGTCACAGAATCATCATA ACA
<i>Rd1 Mutant</i>	GGGTCTCCTCAGATTGATTGA CTAC	GTCACTCTGTGGCCTCAAAGAT
<i>NOD/Scid</i>	TGTAACGGAAAAGAATTGGT ATCCACA	GTTGGCCCCTGCTAACTTTCT

90

91 **Table S4. Reagents used for RNAscope staining.**
 92

Reagents	Dilution	Source	Catalog Number
RNA probes			
PAX2-Hs	No dilution	Advanced Cell Diagnostics	442541
HES6-Hs	1:50	Advanced Cell Diagnostics	521301-C2
ASCL1-Hs	1:50	Advanced Cell Diagnostics	459721-C2
NKX2-2-Hs	No dilution	Advanced Cell Diagnostics	821401
HOXC8-Hs	No dilution	Advanced Cell Diagnostics	506531
ARX-Hs	1:50	Advanced Cell Diagnostics	486711-C2
VSX2-Hs	1:50	Advanced Cell Diagnostics	493031-C2
3-plex positive control-Mm	No dilution	Advanced Cell Diagnostics	320881
3-plex positive control-Hs	No dilution	Advanced Cell Diagnostics	320861
3-plex negative control	No dilution	Advanced Cell Diagnostics	320871
TSA-fluorophores			
TSA plus-Cy3	1:1500	AKOYA Biosciences	NEL744001KT
TSA plus-Cy5	1:1500	AKOYA Biosciences	NEL745001KT

93

94 **Table S5. Antibodies used for RNAscope counterstaining and immunohistochemistry**
 95 **staining.**
 96

Reagents	Dilution	Source	Catalog Number
Primary antibodies			
Rabbit anti-RBPMS	1:500	MilliporeSigma	ABN1362
Mouse anti-NeuN	1:500	MilliporeSigma	MAB377
Mouse anti-Calbindin	1:500	Sigma-Aldrich	C9848
Goat anti-PKC α	1:200	R&D Systems	AF5340
Goat anti-SCGN	1:200	Thermo Fisher Scientific	PA5-47664
Rabbit anti-IBA1	1:250	Abcam	Ab178680
Rabbit anti-CD68	1:100	Abcam	Ab125212
Rabbit anti-Ki67	1:500	Thermo Fisher Scientific	MA5-14520
Rabbit anti-L/M-opsin	1:500	Kerafast	EDK101
Rabbit anti-S-opsin	1:500	MilliporeSigma	Ab5407
Rabbit anti-Rhodopsin	1:500	Abcam	Ab3424
Mouse anti-human nuclear antibody (HNA)	1:1000	MilliporeSigma	Mab1281
Sheep anti-Ki67	1:40	R&D Systems	AF7617
Rabbit anti-Ku80	1:50	Thermo Fisher Scientific	MA5-32212
Secondary antibodies			
Goat anti-Rabbit 488	1:500	Abcam	Ab150077
Goat anti-Mouse 488	1:500	Thermo Fisher Scientific	A-11001
Goat anti-Mouse 647	1:500	Thermo Fisher Scientific	A32728
Donkey anti-Goat 488	1:500	Abcam	Ab150129
Donkey anti-Sheep 647	1:200	Thermo Fisher Scientific	A-21448
Donkey anti-Rabbit 488	1:200	Thermo Fisher Scientific	A21206

97

98 **Supplemental experimental procedures**

99 *Cell Lines*

100 The use of human stem cells was approved by the Johns Hopkins ISCRO (ISCRO00000249). The
101 H9 CRX:tdTomato human embryonic stem cell line (hESCs) was a kind gift from Dr. David M.
102 Gamm (University of Wisconsin Hospitals, USA) and Dr. Donald J. Zack (Johns Hopkins
103 University, USA). The hiPSC line derived from CD34+ cord blood is a commercially available
104 cell line (A18945, Thermo Fisher Scientific)(Burrige et al., 2011). The use of human iPSCs for
105 generation of retinal organoids in this study conforms to the University of Colorado Office of
106 Regulatory Compliance. Stem cells were maintained in mTeSR1 (Stem Cell Technologies,
107 Cambridge, MA, USA) on 1% (vol/vol) Matrigel-GFRTM (BD Biosciences, USA, No. 354230),
108 coated dishes and grown in a 37°C HERAcell 150i incubator at 10%CO₂ and 5% O₂ incubator
109 (Thermo Fisher Scientific, MA, USA). Cells were passaged upon confluence (every 3-6 days)
110 using Accutase (Sigma-Aldrich, MO, USA, No. SCR005) for 7–10 minutes, and dissociated into
111 single cells. Cells in Accutase were added 1:2 to mTeSR1 plus 5 μM Blebbistatin (Bleb; B0560,
112 Sigma), pelleted at 700 g for 5 minutes, and suspended in mTeSR1 plus Bleb and plated at 5,000
113 cells per well in a six-well plate. After 48 hours, cells were fed with mTeSR1 (without Bleb) every
114 24 hours until the next passage. To minimize cell stress, no antibiotics were used in RPMI (Gibco,
115 USA) and supplement media (10% fetal bovine serum (FBS), 2.5% penicillin). Cells were
116 maintained at 37°C and 5% CO₂ and passaged every 3-4 days at $\sim 1 \times 10^5 - 2 \times 10^6$ cells/ml in
117 uncoated flasks. Cells were routinely tested for mycoplasma using MycoAlert (Lonza, Switzerland,
118 No. LT07).

119 ***Retinal organoid culturing***

120 For H9 CRX:tdtomato⁺ retinal organoid culturing, the hESCs were dissociated in Accutase at 37°C
121 for 12 min and seeded in 50 µl of mTeSR1 at 3,000 cells/well into 96-well ultra-low adhesion
122 round bottom Lipidure coated plates (AMSBIO, MA, USA, No.51011610). Cells were placed in
123 hypoxic conditions (10% CO₂ and 5% O₂) for 24 hours to enhance survival. Cells naturally
124 aggregated by gravity over 24 hours. On day 1, cells were moved to normoxic conditions (5%
125 CO₂). On days 1- 3, 50 µl of BE6.2 media, **Table S1**) containing 3 µM Wnt inhibitor (IWR1e,
126 EMD Millipore, MA, USA, No. 681669,) and 1% (v/v) Matrigel were added to each well. On days
127 4-9, 100 µl of media were removed from each well, and 100 µl of media were added. On days 4-
128 5, BE6.2 media containing 3 µM Wnt inhibitor and 1% Matrigel was added. On days 6-7, BE6.2
129 media containing 1% Matrigel was added. On days 8-9, BE6.2 media containing 1% Matrigel and
130 100 nM Smoothened agonist (SAG, EMD Millipore, No. 566660) was added. On day 10,
131 aggregates were transferred to 15 mL tubes, rinsed 3X in DMEM (Gibco, No. 11885084), and
132 resuspended in BE6.2 with 100 nM SAG in untreated 10 cm polystyrene petri dishes. From this
133 point on, media was changed every other day. Aggregates were monitored and manually separated
134 if stuck together or to the bottom of the plate. On day 11, retinal vesicles were manually dissected
135 using sharpened tungsten needles. After dissection, cells were transferred into 15 mL tubes and
136 washed 2X with 5 mLs of DMEM. On days 14-17, long-term retina (LTR, **Table S1**) media with
137 100 nM SAG was added. On days 18-21, cells were maintained in LTR and washed 2X with 5
138 mLs of DMEM, before being transferred to new plates to wash off dead cells. To increase survival
139 and differentiation, 1 µM all-trans retinoic acid (ATRA; R2625; Sigma) was added to LTR
140 medium from days 22-138. 10 µM Gammasecretase inhibitor (DAPT, EMD Millipore, No. 565770)
141 was added to LTR from days 28-42. Retinal organoids were grown at low density (10-20 per 10
142 cm dish) to reduce aggregation.

143 For the generation of retinal organoids from human iPS cells, a human induced pluripotent
144 stem cell (hiPSC) line derived from CD34⁺ cord blood was used for all experiments in this study
145 (A18945, ThermoFisher Scientific) (Burrige *et al.*, 2011). Cell culture, retinal differentiation, and
146 human retinal organoid formation were conducted as previously described (Zhong *et al.*, 2014). A
147 more detailed protocol of the methodology for generating retinal organoids was recently described
148 (Aparicio-Domingo *et al.*, 2023). Briefly, hiPSCs were maintained on Matrigel (growth-factor-
149 reduced; BD Biosciences) coated plates. After 6 days in culture, hiPSC colonies were lifted and
150 cultured as free-floating neural aggregates (NAs); this was established as Day 0 (D0) of
151 differentiation. On D7, NAs were seeded onto Matrigel (growth-factor-reduced; BD Biosciences)
152 coated dishes, and individual mechanical detachment of the NR and RPE domains was performed
153 between D21 and D23. The culture media and reagents are listed in **Table S2**. Undifferentiated
154 hiPSCs and derived retinal organoids were routinely tested for Mycoplasma contamination by PCR.

155 *Animals*

156 All animal experiments were carried out in accordance with the ARVO Statement for the Use of
157 Animals in Ophthalmic and Vision Research. All procedures were approved by the Johns Hopkins
158 University Animal Care and Use Committee (approval M016M17). The C3H/HeJ-*Pde6*^{Rd1/Rd1}
159 (referred to as *Rd1*), and NOD.Cg-*Prkdc*^{scid}/J (referred to as *NOD/Scid*) mice of either gender (aged
160 6 to 8 weeks) were obtained from Jackson Laboratory (Bar Harbor, ME, USA). All mice were
161 housed in cages under a 12:12-hour light-dark cycle with water and food provided *ad libitum*.

162 *Recipient mice*

163 We created a recipient mouse model with immune-deficiency and retinal degeneration (referred to
164 as *Rd1/NS*) by crossbreeding *Rd1* mice and *NOD/Scid* mice (aged 8 weeks). The breeding strategy
165 was performed as previously reported (Wenzel *et al.*, 2007). Genomic DNA of the third-generation

166 offspring was extracted from ear biopsies and genotyped by Transnetyx Tag Center (Cordova, TN,
167 USA). Primers were listed in **Table S3**. Eyes of adult *Rdl/NS* mice (n=3) were collected to
168 characterize photoreceptor degeneration using immunohistochemistry (IHC) staining, as
169 previously reported (Liu et al., 2021). Flow cytometry was performed using spleen biopsies of
170 adult *Rdl/NS* mice (n=3) to confirm the deficiency of T cells and B cells, as previously described
171 (Hensel et al., 2019). Phenotyping data of *Rdl/NS* mice are shown in **Fig. S1**.

172 ***Preparation of donor cells***

173 Donor retinal organoid cells (harvested as micro-dissected multilayered retinal fragments) were
174 obtained from CRX:tdTomato⁺ hESC-derived retinal organoids (aged 134 days, n=4) and hiPSC
175 derived retinal organoids (aged 150 days, n=3). The cultured human retinal organoids were imaged
176 using a fluorescent microscope (Carl Zeiss, Jena, Germany). The images were used as a reference
177 to isolate the retinal cluster from the donor retinal organoids. The isolated retinal organoids clusters
178 were then cut into 1 × 1 mm² or 1 × 2 mm² microdissected fragments using a 27-gauge horizontal
179 curved scissors (VitreQ, Kingston, NH, USA) under a dissection microscope. Donor cells were
180 transplanted within two hours of isolation.

181 ***Transplantation of donor cells***

182 Donor retinal organoid fragments were transplanted into the subretinal space of *Rdl/NS* mice (aged
183 6 to 8 weeks, n=16 eyes for hESC-derived retinal organoids, n=5 eyes for iPS-derived retinal
184 organoids), as previously reported (Liu et al., 2020). Briefly, recipient mice were anesthetized by
185 intraperitoneal injection of ketamine (100 mg/kg body weight) and xylazine hydrochloride (20
186 mg/kg body weight). Mouse pupils were dilated with 1% (wt/vol) tropicamide (Bausch & Lomb,
187 Rochester, NY, USA). Mouse corneas were covered with Sodium Hyaluronate (Healon GV,
188 Abbott Medical Optics Inc. CA, USA) and cover glasses (Deckglaser, USA) to facilitate

189 transpupillary visualization. The donor retinal organoid fragments were loaded into the bevel of a
190 26G microneedle with the photoreceptor side facing down, gently aspirated into the attached
191 micro-syringe (Hamilton, Reno, NV, USA), then tangentially injected into the subretinal space
192 through the sclera of the recipient mice. Successful injection was verified by direct visualization
193 through the dilated pupil of the recipient under the surgical microscope (Leica, Wetzlar, Germany).

194 *Single cell RNA sequencing*

195 Single cell RNA sequencing (scRNA-seq) was performed on dissociated cells from transplanted
196 and cultured CRX:tdTomato⁺ retinal organoids using the Chromium platform (10X Genomics).
197 Briefly, retinal organoid cells were dissociated into a single cell suspension using the Papain
198 Dissociation System (Worthington) for 60 minutes at 37°C, with gentle mixing every 5 minutes,
199 before stopping the reaction using ovomucoid protease inhibitors. Cells were centrifuged and
200 resuspended in ice-cold PBS containing 0.04% bovine serum albumin (BSA) and 0.5 U/ μ l RNase
201 inhibitor and were filtered through a 40- μ m Flowmi cell strainer (Bel-Art SP). Cell counts and
202 viability were assessed by Trypan blue staining before loading 6000 cells on a Chromium Single
203 Cell system using Next GEM 3' reagent v3.1 kits. Libraries were pooled and sequenced on
204 Illumina NextSeq 500 with ~50,000 reads per cell. The Cell Ranger 4 (10X Genomics) pipeline
205 was used to process the raw sequencing reads for demultiplexing. Since the starting material used
206 to generate the library consisted of human and mouse cells, reads were aligned to a hybrid
207 GRCm38 mouse and GRCh38 human reference genome. Cell barcodes that had most of their reads
208 mapped to GRCm38 mouse genes were considered to be of mouse origin and excluded. The
209 remaining cellular barcode-associated reads were re-mapped to the GRCh38 human reference
210 genome and a cell-by-gene count matrix was generated for downstream analysis. In this study,
211 only the human cells were ultimately analyzed. The generated cell-by-gene count matrices were

212 analyzed using the Seurat ver3 R package (Stuart et al., 2019). We filtered out cells that had UMIs
213 less than 300 or greater than 50000 and with a mitochondrial fraction of greater than 20%. Doublets
214 were identified and removed using the DoubletFinder R package (McGinnis et al., 2019). Log-
215 normalization, scaling, UMAP dimensional reduction and clustering were performed using the
216 standard Seurat pipeline. Quality control of scRNA-seq data were shown in **Fig. S6**. Major retinal
217 cell types were identified using previously identified cell type markers (Hoang et al., 2020).
218 Enriched genes from the brain/spinal-like cell cluster were compared to the ASCOT (Ling et al.,
219 2020) gene expression summaries of public RNA-Seq data to determine its classification.
220 Differential gene tests were performed by Seurat's *FindMarkers* function using the Wilcoxon rank
221 sum test with default parameters (Stuart *et al.*, 2019). Hierarchical clustering was used to group
222 the differentially expressed genes. The UCell R package (Andreatta and Carmona, 2021) was used
223 to calculate the migration potential score or the proliferation score (**data files S1, S2**). The gene
224 sets were constructed by identifying enriched genes within the gene ontology terms cell migration
225 and cell motility for the migration potential score and cell division for the proliferation score
226 respectively. The Seurat integration functions (*SelectIntegrationFeatures*,
227 *FindIntegrationAnchors* and *IntegrateData*) were used to integrate the organoid data onto the
228 human retinal developmental dataset (Lu et al., 2020). Monocle 3 (Cao et al., 2019) was used to
229 perform pseudotime analysis and identify trajectory routes within the data.

230 ***Histology***

231 Four and a half months post-transplantation, the recipient mice were sacrificed with over-dose
232 anesthesia and pre-fixed by heart-perfusion with 4% paraformaldehyde (PFA) (Electron
233 Microscopy Sciences, Hatfield, PA, USA) in PBS. Eyes were gently removed, post-fixed in 4%
234 PFA/PBS for one hour at room temperature (RT), and dehydrated in a sucrose gradient (10%, 20%,

235 30%), then blocked in optimal cutting temperature compound (Sakura Finetek, Torrance, CA,
236 USA). Cultured retinal organoids were fixed in 4% PFA at RT for 15 minutes (min), dehydrated
237 in gradient sucrose (10%, 20%, 30%), and blocked in the OCT compound. OCT-blocked recipient
238 mouse eyes and cultured retinal organoids were cut into 7-10 μm thick cryosections using a
239 microtome (CM 1850; Leica) for histological staining.

240 RNAscope and IHC counter-staining was performed according to the manufacturer's
241 protocol (Advanced Cell Diagnostics (ACD), see Protocol #MK 51-150, Appendix D.). Briefly,
242 cryosections of recipient mice eyes and cultured retinal organoids were rinsed with PBS, baked in
243 a HyBEZTM oven (ACD, USA) for 30 min at 60°C, and post-fixed in pre-chilled 4% PFA in PBS
244 for 15 min at 4°C. Slides were dehydrated in gradient ethanol (50%, 70%, 100%), treated with
245 hydrogen peroxide (10 min at RT), then subjected to target retrieval using the Co-detection Target
246 Retrieval solution (ACD, Cat. No. 323180) at 98-102°C for 5 min. After rinsing in distilled water
247 (2 min x 2) and PBS-T (5 min x 1), the slides were incubated with diluted primary antibody at 4°C
248 overnight. On day 2, slides were post-fixed with 4% PFA for 30 min at RT, treated with protease
249 III at 40°C for 30min, and subjected to RNAscope staining using the RNAscope Multiplex
250 Fluorescent V2 assay according to the manufacturer's protocol (ACD, RNAscope USM-323100,
251 see "fixed-frozen tissue sample protocol"). Briefly, RNA probe hybridization was performed with
252 the HyBEZTM oven for two hours at 40°C. Slides were then assigned for three series of
253 amplification, fluorochromes combination, and HRP blocking. After the RNAscope procedure,
254 slides were incubated with secondary antibody at RT for one hour, counter stained with DAPI, and
255 mounted with Prolong Diamond (Life Technology, Carlsbad, CA, USA). The RNA probes,
256 fluorophores used were listed in **Table S4**. The primary and secondary antibodies used for IHC

257 counter staining were listed in **Table S5**. Negative and positive multiplex control probes staining
258 were run in parallel with the target probes following the same protocol (data shown in **Fig. S7**).

259 IHC staining was performed as previously described (Liu *et al.*, 2020). Briefly,
260 cryosections of transplanted *Rdl/NS* mice and cultured retinal organoids were rinsed with PBS (5
261 min x 1), permeabilized, and blocked with a mixture of 0.1% Triton-X100 and 5% goat serum in
262 PBS for one hour at RT. The slides were rinsed in PBS (5 min x 3), incubated with primary
263 antibodies at 4°C overnight, incubated with secondary antibodies at RT for one hour, then counter
264 stained with DAPI and mounted using ProLong Diamond mounting media. The primary antibodies
265 and secondary antibodies used here were listed in **Table S5**.

266 ***Quantification of donor cell migration of recipient retina***

267 For migratory distance quantification of transplanted retinal organoid cells, retinal sections from
268 recipient mice were stained with human nuclear specific antibodies HNA (Sigma-Aldrich, MO,
269 USA) or Ku80 (Thermo Fisher Scientific, MA, USA). Tile scan images were collected using
270 Confocal LSM 880 (Zeiss, Oberkochen, Germany) for distance quantification. The migratory
271 distance of transplanted retinal organoids was defined as the shortest distance between the
272 migratory cells and the nearest graft edge (i.e., the graft-left migratory cells to the left endpoint of
273 the graft; the graft-right migratory cells to the right endpoint of the graft). We used a mathematical
274 method to facilitate distance quantification. Specifically, the graft edge was defined as a “starting
275 point” and the migratory cells in different retinal laminae (RGC, IPL, INL, RPE/C) were manually
276 targeted, both processed with the “Cell Counter” plugin in ImageJ. The cell coordinates were
277 automatically collected to quantify the X and Y axial distances of individual cells by the Cell
278 Counter. The axial distance of the graft edge (starting point) was referred to as “X_{start}” and “Y_{start}”.
279 The axial distance of the migratory cells was referred to as “X_{migratory}” and “Y_{migratory}”. The

280 migratory distance was computed in R platform (see supplementary **coding file S1**) following the
281 formula:

$$282 \quad \text{Migrating distance} = \sqrt{(X_{start} - X_{migratory})^2 + (Y_{start} - Y_{migratory})^2}$$

283 The unit of the migrating distance was converted from pixel to micron according to the image
284 scale.

285 For cell quantification, the number of positively stained cells was manually counted using
286 the “Cell Counter” plugin in ImageJ. The representative pre-synapse graphs of the transplanted
287 and cultured retinal organoids were drawn by Imaris software (Version 9.5.0, Bitplane AG, Zurich,
288 Switzerland).

289 *Electrophysiology*

290 The electrophysiological recording was performed on the transplanted CRX:tdTomato⁺
291 photoreceptors eight months post-transplantation to measure their physiological properties. We
292 were able to test only one recipient mouse (the second recipient mouse died before the assay during
293 the long-term observation). The recipient's eyes were gently pulled out from the recipient mouse
294 and put in Ames' medium (Sigma No. A1420). Retinas with transplanted retinal organoids were
295 dissected by removing the corneas and lens under infrared light, attached to a piece of filter,
296 sectioned into 200µm slices, and transferred to a recording chamber. The CRX:tdTomato⁺
297 photoreceptors of the transplanted retinal organoids were targeted under an epifluorescence
298 microscope for consequent whole-cell patch-clamp recording. Fluorescent signal was imaged by
299 a Nikon CCD camera with data acquisition synchronized with a 20-ms flash of epi-fluorescence
300 excitation light. The total exposure time to excitation light before recording was <500 ms. During
301 recording, retina was perfused with Ames' medium bubbled with 95% O₂/5% CO₂. Patch
302 electrodes (5-7 MΩ) were pulled from borosilicate capillaries (GC150-10, Harvard Apparatus) and

303 filled with an internal solution containing typically (in mM): 120 K-gluconate, 5 NaCl, 4 KCl, 10
304 HEPES, 2 EGTA, 4 ATP-Mg, 0.3 GTP-Na₂, and 7 Phosphocreatine-Tris, with pH adjusted to 7.3
305 with KOH. Whole-cell patch-clamp recording was made at 30–32°C with an Axon Instruments
306 Multiclamp 700B amplifier. Series resistance of patch electrodes was 10–30 MΩ. Liquid-junction
307 potential (measured to be -13 mV) has been corrected. In voltage-clamp mode, recorded cells were
308 held at -40 mV, followed by voltage steps of 100-ms (-70 mV to -10 mV). All procedures were
309 carried out in the darkroom to avoid photoreceptor bleaching.

310 *Statistical analysis*

311 Quantitative histology data were analyzed using two-way ANOVA. Sidak's test or Tukey's test
312 was adopted for multiple comparisons (two-tailed). Independent T-test or Mann-Whitney U test
313 was used for two variants comparison. Statistical analysis was carried out using SPSS software
314 (version 25, IL, USA). $p < 0.05$ was taken to be significant. Statistical data were presented as mean
315 \pm SD. Graphs were drawn with GraphPad Prism software (version 8, CA, USA). Schematics were
316 created with BioRender.com (agreement number QH23QWJX12, KY23QWKEPB).

317 Supplemental References

- 318 Andreatta, M., and Carmona, S.J. (2021). UCell: Robust and scalable single-cell gene signature
319 scoring. *Comput Struct Biotechnol J* 19, 3796-3798. 10.1016/j.csbj.2021.06.043.
- 320 Aparicio-Domingo, S., Flores-Bellver, M., Cobb, H., Li, K.V., Conrad, B., Chen, C., Brzezinski,
321 J.A., and Canto-Soler, M.V. (2023). Generation of Three-Dimensional Retinal Tissue with
322 Physiologically Competent, Light-Sensitive Photoreceptors from Human-Induced Pluripotent
323 Stem Cells. In *Brain Organoid Research*, J. Gopalakrishnan, ed. (Springer US), pp. 99-119.
324 10.1007/978-1-0716-2720-4_6.
- 325 BurrIDGE, P.W., Thompson, S., Millrod, M.A., Weinberg, S., Yuan, X., Peters, A., Mahairaki, V.,
326 Koliatsos, V.E., Tung, L., and Zambidis, E.T. (2011). A universal system for highly efficient
327 cardiac differentiation of human induced pluripotent stem cells that eliminates interline
328 variability. *PLoS One* 6, e18293. 10.1371/journal.pone.0018293.
- 329 Cao, J., Spielmann, M., Qiu, X., Huang, X., Ibrahim, D.M., Hill, A.J., Zhang, F., Mundlos, S.,
330 Christiansen, L., Steemers, F.J., et al. (2019). The single-cell transcriptional landscape of
331 mammalian organogenesis. *Nature* 566, 496-502. 10.1038/s41586-019-0969-x.
- 332 Hensel, J.A., Khattar, V., Ashton, R., and Ponnazhagan, S. (2019). Characterization of immune
333 cell subtypes in three commonly used mouse strains reveals gender and strain-specific variations.
334 *Lab. Invest.* 99, 93-106. 10.1038/s41374-018-0137-1.
- 335 Hoang, T., Wang, J., Boyd, P., Wang, F., Santiago, C., Jiang, L., Yoo, S., Lahne, M., Todd, L.J.,
336 Jia, M., et al. (2020). Gene regulatory networks controlling vertebrate retinal regeneration.
337 *Science (New York, N.Y.)* 370. 10.1126/science.abb8598.
- 338 Ling, J.P., Wilks, C., Charles, R., Leavey, P.J., Ghosh, D., Jiang, L., Santiago, C.P., Pang, B.,
339 Venkataraman, A., Clark, B.S., et al. (2020). ASCOT identifies key regulators of neuronal
340 subtype-specific splicing. *Nat Commun* 11, 137. 10.1038/s41467-019-14020-5.
- 341 Liu, Y.V., Sodhi, S.K., Xue, G., Teng, D., Agakishiev, D., McNally, M.M., Harris-Bookman, S.,
342 McBride, C., Konar, G.J., and Singh, M.S. (2020). Quantifiable in vivo imaging biomarkers of
343 retinal regeneration by photoreceptor cell transplantation. *Transl. Vis. Sci. Technol.* 9, 5.
344 10.1167/tvst.9.7.5.
- 345 Liu, Y.V., Teng, D., Konar, G.J., Agakishiev, D., Biggs-Garcia, A., Harris-Bookman, S.,
346 McNally, M.M., Garzon, C., Sastry, S., and Singh, M.S. (2021). Characterization and allogeneic
347 transplantation of a novel transgenic cone-rich donor mouse line. *Exp. Eye Res.* 210, 108715.
348 10.1016/j.exer.2021.108715.
- 349 Lu, Y., Shiau, F., Yi, W., Lu, S., Wu, Q., Pearson, J.D., Kallman, A., Zhong, S., Hoang, T., Zuo,
350 Z., et al. (2020). Single-cell analysis of human retina identifies evolutionarily conserved and
351 species-specific mechanisms controlling development. *Dev. Cell* 53, 473-491.e479.
352 10.1016/j.devcel.2020.04.009.
- 353 McGinnis, C.S., Murrow, L.M., and Gartner, Z.J. (2019). DoubletFinder: Doublet Detection in
354 Single-Cell RNA Sequencing Data Using Artificial Nearest Neighbors. *Cell Syst* 8, 329-337
355 e324. 10.1016/j.cels.2019.03.003.
- 356 Stuart, T., Butler, A., Hoffman, P., Hafemeister, C., Papalexi, E., Mauck, W.M., 3rd, Hao, Y.,
357 Stoeckius, M., Smibert, P., and Satija, R. (2019). Comprehensive Integration of Single-Cell Data.
358 *Cell* 177, 1888-1902 e1821. 10.1016/j.cell.2019.05.031.
- 359 Wenzel, A., von Lintig, J., Oberhauser, V., Tanimoto, N., Grimm, C., and Seeliger, M.W.
360 (2007). RPE65 is essential for the function of cone photoreceptors in NRL-deficient mice. *Invest.*
361 *Ophthalmol. Vis. Sci.* 48, 534-542. 10.1167/iovs.06-0652.

362 Zhong, X., Gutierrez, C., Xue, T., Hampton, C., Vergara, M.N., Cao, L.H., Peters, A., Park, T.S.,
363 Zambidis, E.T., Meyer, J.S., et al. (2014). Generation of three-dimensional retinal tissue with
364 functional photoreceptors from human iPSCs. Nat Commun 5, 4047. 10.1038/ncomms5047.
365

366

367 **Supplemental coding file S1**

368 **R coding algorithms for migrating distance quantification**

```
369 library(data.table)
370 library(plyr)
371
372 #####
373 #
374 # Extract the X,Y coordinate of migrated cells, and generate subsequent distance data presented in
375 Table 1
376 #
377 #####
378
379 #---> Extracting data exported from ImageJ
380
381 common_path = "~/Desktop/cell invasion/Processed_Image"
382
383 files_to_read = list.files(
384   path = common_path,      # directory to search within
385   pattern = ".*(Rd1-NS).*csv$", # regex pattern
386   recursive = TRUE,       # search subdirectories
387   full.names = TRUE       # return the full path
388 )
389
390 #---> Hypothetical Researcher has 37 retina slides to quantify
391 #   and wants to localize 5 cell types per retina slides. So that's
392 #   37 rows and 6 columns (including cell id) in the data list
393
394 data_lst = lapply(files_to_read, read.csv) # read all the matching files
395 celltype_summary = data.frame(matrix(ncol = 6, nrow = 37))
396 colnames (celltype_summary) <- c("File_name", "Type_1", "Type_2", "Type_3", "Type_4",
397 "Type_5")
398
399 #---> Calculating the distance from starting point for each cell
400 #   categorized by cell types
401
402 for (i in 1:length(data_lst)){
403   data_lst[[i]]$Address <- rep(files_to_read[i],nrow(data_lst[[i]]))
```

```

404 File_Name <- files_to_read[i]
405 Type_1 <- sum(data_lst[[i]]$Type == 1)
406 Type_2 <- sum(data_lst[[i]]$Type == 2)
407 Type_3 <- sum(data_lst[[i]]$Type == 3)
408 Type_4 <- sum(data_lst[[i]]$Type == 4)
409 Type_5 <- sum(data_lst[[i]]$Type == 5)
410 celltype_summary[i,1:6] = c(File_Name, Type_1, Type_2, Type_3, Type_4, Type_5)
411 print(c(File_Name, Type_1, Type_2, Type_3, Type_4, Type_5))
412 for (j in 1:nrow(data_lst[[i]])){
413   data_lst[[i]][j,"Z.µm."]=sqrt(( data_lst[[i]][j,"X.µm."]- data_lst[[i]][1,"X.µm."])^2 +
414     ( data_lst[[i]][j,"Y.µm."]- data_lst[[i]][1,"Y.µm."])^2) #distance calculation
415 }
416 }
417
418 #---> Exporting analyzed invasion distance summary
419
420 dat1<-ldply(data_lst)
421
422 write.table(as.data.frame(dat1),file="Detialed_Result.csv", quote=F,sep="," ,row.names=F)
423 write.table(as.data.frame(celltype_summary),file="Celltype_Summary.csv",
424   quote=F,sep="," ,row.names=F)

```